Effect of oxidation post treatments on TiO2 coating manufactured using reactive very low-pressure plasma spraying (R-VLPPS)

X. Fan, M.-P. Planche, G. Darut, H. Liao, G. Montavon, J. Ilavsky

Effect of oxidation post treatments on TiO_2 coating manufactured using reactive very low-pressure plasma spraying (R-VLPPS)

X. Fan, M-P. Planche, G. Darut, H. Liao, G. Montavon

ICB UMR 6303, CNRS, Université de Bourgogne Franche-Comté, UTBM, 90010 Belfort, France
marie-pierre.planche@utbm.fr

J. Ilavsky
Advanced Photon Source, Argonne National Laboratory, 9700 S. Cass Avenue, Argonne, IL 60439, USA

Abstract

TiO_2 coatings manufactured using reactive very low-pressure plasma spraying (R-VLPPS) were analyzed in different regions related to their position compared to the plasma flame. For that, a screen was used in order to hide an area of the substrate from the direct plasma flux. The coating morphology changed from quasi lamellar structure to highly vapor structure and coatings exhibited obvious modifications in terms of phases and mechanical properties. The effect of oxidation post treatment on the as sprayed coating was then studied by selecting two methods: in situ oxidation post treatment and classical thermal treatment. The two post treatments provided an increase of the main rutile phase and a decrease of both the size and the contents of porosity simultaneously.

Keywords: very low-pressure plasma spraying; rutile TiO_2 coating; microstructure; vapor condensation; oxidation post treatment

1 Introduction

Regarding thermal plasma spraying, the development of the specific VLPPS technology (1 ~ 2 mbar, [1, 2]) is extremely challenging in terms of structure that can be formed [3, 4]. Indeed, due to the high plasma energy and the low pressure of such technology, the coating mechanisms exhibit similar behaviors to APS, PVD and CVD leading to spray liquid and vapor phases simultaneously [5]. The plasma flow expands at the exit of the torch to form a jet of about 1m long, characteristic value. This process is based on a different deposition mechanism, regarding to conventional plasma spraying, either at atmospheric pressure (for APS) or at low pressure (20000 Pa, characteristic value for VPS): the coating is manufactured, pass by pass, mostly by the condensation of vapors instead of the solidification of molten particles. Indeed, feedstock particle vaporization occurs in the plasma core, at the exit of the torch. The coating includes lamellar structure, vapor structure and a mix of the two. To date, current studies mostly focus on the manufacturing of ceramic or metallic coatings. This process is currently used to spray metallic coatings such as Al, Cu and Ti for SOFC, electronic devices or additive manufacturing areas [6-8].

Reactive – very-low pressure plasma spraying (R-VLPPS) opens a potential regarding the long dwell-time of the vapors to induce their reaction with a gaseous precursor, injected in the plasma flow either as plasma forming gas and/or downstream the plasma flow to form, in situ, new species that condense onto the substrate. It consists in inducing reactions between a precursor and a reactive gas to form non-congruent melting materials. The option is then to consider a pure metallic powder and a reactive precursor to form in situ composites. R-VLPPS is implemented to obtain most of the nitrides, most of the silicates, numerous carbides or oxides as well [9-10] in order to circumvent the drawback of spraying non-congruent melting materials. Among these materials, TiO_2 is widely known as an excellent semiconductor, photocatalytic, optical and medical material [11-13]. Three kinds of

crystalline phases (anatase, rutile and brookite) exist and the rutile structure is thermodynamically more stable than the others [14]. Numerous techniques are used to elaborate this material but none of them can be considered as the best to synthesis crystalline phases of TiO_2 due to polluted traces or economical reasons or need of additional techniques [15-17]. For example, the enhancement of mechanical properties of TiO_2 coatings such as tribological properties were studied by adding an oxidation post treatment [18-19]. Results showed the presence of the rutile phase layer on the top of the coating providing increased corrosion resistance or hardness.

This work aims at preparing TiO_2 coatings by R VLPPS method. The interest in the use of R-VLPPS method relies on its efficiency to produce large area of non-contaminated coatings in a relatively short time. Particularly, different coating structure can be obtained depending on the position of the substrate relatively to the plasma jet. At first, the microstructure of the coating was investigated by the use of an adapted screen placed front of the substrate. This way, coating morphology and thickness can be studied related to the substrate position. Then, the effect of in situ R-VLPPS post treatment was applied to change contents and phases in the as sprayed coating. This in situ oxidation post treatment method was finally compared to classical oxidation post treatment. The comparison of the post treated coating properties was discussed.

2 Experimental

2-1 Material and process

For the preparation of TiO_2 coatings, a 99,99 at. % of pure Ti powder (AP&C, Canada) with 7-23µm size distribution was used. Its morphology was spherical and its mean diameter was about 13µm as shown in Fig 1. Priori to spraying, rectangular shape (4*10*2mm) of stainless steel substrates were grit blasted and cleaned by acetone. Experiments were carried out in a VLPPS system developed in-house, composed of a 12 m^3 water cooled vacuum chamber

equipped with the commercial 50kW Oerlikon-Metco F4-VB type plasma torch fixed on a 6-axis robot. Optimized VLPPS plasma parameters of 700A current intensity, 50 kW power and 45/12L/min Ar/H_2 as forming gas were selected for manufacturing the coatings under 150Pa. Two different altrenatives were considered to inject the reactive species, Oxygen, in the plasma flow. The first way considers oxygen injected in the torch nozzle just before the anode exit. The torch scans the surface during the post treatment without changing the spray distance and removing the screen. The second way uses a ring-shaped injector located downstream, close to the substrate surface. This way, the additional O_2 reactive gas was injected within the primary gas mixture to initiate chemical reactions during the particle travelling and near the substrate to reinforce the oxidation mechanisms during the impact of the sprayed powder. The flowrate of O_2 gas was 4L/min each.

To investigate the changes in TiO_2 microstructures, the following screen was adjusted to distinguish three different coating formation, Fig 2:

Area FRONT (F), Front of the plasma jet;

Area INTERMEDIATE (I), Intermediate stage between the direct and the hidden spray;

Area HIDDEN (H), completely Hidden from the plasma jet.

Detailed results given in a previous study [20] showed the benefits of longer interactions time, moderate substrate temperature for reaching the highest rutile TiO_2 phase in the coating about 84%. Based on these results, oxidation post treatment was applied on the formed coating in order to increase the rutile phase. The first oxidation post treatment consisted of applying to an elaborated TiO_2 coating a relatively larger quantity of reactive gas in the plasma jet without powder (in situ R-VLPPS post treatment, 8L/min O_2). Working conditions are given in Table 1. The second consisted of submitting the as sprayed coating to a classical Thermal Post Treatment. Previous studies have been conducted to optimize both, the temperature and the

exposure time of the coating oxidation in the oven. Results showed the best oxidation for 550°C and 4 hour exposure. TiO_2 coating properties were separately analysed and compared.

2-2 Characterization

Changes in microstructure, phases and contents, were successively characterized by optical microscopy (EPIPHOT, Nikon, Japan), X-ray diffraction (BRUKER, United States), and scanning electron microscopy (JEOL, Japan). Mechanical properties were calculated through Vickers (Leitz, Germany) and nanoindentation measurements (HYSITRON, United States). 10 measures were randomly performed to provide a mean value and a standard deviation of Hardness and Young Modulus of the coatings.

X-ray transmission technique (Argonne National Laboratory, Argonne, IL, USA) was applied to analyze the total porosity of the as prepared coatings as it has a resolution down to 1 µm. Since the density and chemical composition of the free-standing coatings are known, linear absorption coefficient of the X-rays through the solid phase can be calculated using theoretical models [21].

3 Results

3.1 In situ oxidation post treatment using reactive VLPPS mode (R-VLPPS)

The microstructures of the cross section of FRONT, INTERMEDIATE and HIDDEN zones are displayed in Fig 3. Moving from a visible to a hidden area of the substrate compared to the spray jet, the lamellar microstructure was totally transformed into a vapor microstructure leading to decrease by more than 30 times the coating thickness. The contrast due to the lamellar structure in FRONT zone (dark grey for TiO_2) is no longer observable in HIDDEN zone where the columnar structure was reached. In FRONT region (direct spray), the coating exhibits a mixed microstructure of spread lamellae and condensed vapors (light gray and dark gray contrasts, respectively) identical to that of the coating without thermal oxidation

treatment. The dark gray areas are due to TiO_2 phase. In IINTERMEDIATE region (border between direct spray and masked spray), the thickness of the deposit has greatly decreased from 70 to 40 µm µm due to the presence of the mask which reduces the number of particles impacting on the surface. The corresponding coating has a microstructure with fewer lamellae (light gray contrast). In HIDDEN region (masked spray), the deposit is composed only of vapor condensation (no light gray contrast linked to the spread molten particles). It consists of a dense columnar microstructure and a relatively small thickness (about 3µm). The EDS analysis of the FRONT and HIDDEN areas confirmed the different phases of Ti and O elements Fig 4. In FRONT zone, the mass ratio of Ti oscillated from the highest value found in lamellar structure (88%) to a significantly lower value for columnar structure (67%). When the analysis line passes over a spreading lamella, the element Ti increases to 88% against 12% for O. When the analysis line passes over condensed vapors, the element Ti passes to 67% against 33% for O. Instead, in HIDDEN zone, the mass ratio of O continuously decreased due to oxidation post treatment involving at the surface mostly (from 45% to 28%). This comes from the in-situ oxidation heat treatment which promotes the concentration of reactive oxygen on the surface of the coating. At the same time, it should be noted that the elements Fe, Ni, Cr constituting the substrate have diffused into the HIDDEN region. This indicates that an apparent metallurgical bond exists between the coating and the substrate which is beneficial for the adhesion.

In addition, the microstructures of the coating surfaces were analyzed for these same two regions, Fig 5. In FRONT region, the surface topography reveals the impact and crushing of molten particles on the surface of the substrate. We also note the presence of some spherical particles of about 4µm included within the vapors. In HIDDEN region, the surface of the coating consists of a large quantity of ultrafine particles with a size less than 300nm. Some are

agglomerated into particles larger than a few micrometers. These stacks come from the condensation of vapors and agree with the previous comments.

Figure 6 shows the EDS chemical analyzes carried out on the surface in FRONT and HIDDEN regions. The elementary phase of both regions corresponds to Ti and O elements. The mass fraction of the oxygen element in the coating of HIDDEN region is greater than that of FRONT region. The coating in HIDDEN region is composed entirely of vapors. The oxidation reaction between the Ti vapors and the oxygen will be optimized compared to a more massive liquid particle. More TiO_2 phase will be generated in that case.

XRD pattern of FRONT, INTERMEDIATE and HIDDEN zones are shown in Fig.7. Compared to XRD pattern of the as sprayed coating, the intensity of the TiO_2 peaks confirms the efficiency of the in-situ post treatment. The unique TiO_2 rutile phase was detected in the HIDDEN columnar coating reflecting its crystallographic purity. TiO_2, Ti_2O and Ti_3O peaks were found in both, FRONT and INTERMEDIATE lamellar coatings whose intensities varied with the amount of vapor phase. Other peaks appear on the pattern and are likely attributed to Ti_xO_y phases. For conventional thermal spray coatings, manufactured from micrometer or nanometer sized particles [23,24], anatase and rutile TiO_2 are obtained. Also Magneli, Ti_3O_5 [25] and Ti_2O_3 phases can be formed with H_2 plasma forming gas use [26]. Ti_2O and Ti_3O phases seems to have never been observed previously in coatings. Only some papers on mechanical properties of titanium oxides discussed on this phases [27]. The diffraction peaks were used to determine the average ratio of each phase based on Rietveld analysis. Quantitative results are shown in Table 2. Obtained results are consistent with the EDS analysis. The average ratio of TiO_2 is quite close to 100% for HIDDEN and decreases progressively from INTERMEDIATE to FRONT due to the loss of vapor contents. In that cases, TiO_2 is gradually replaced by Ti_2O and Ti_3O.

Results of the porosity contents show a progressive decrease from 10%, the highest value for lamellae coating (i.e FRONT zone) to 3% for columnar structure (i.e. HIDDEN zone), Fig 8. However, the quantity of the small pores less than 2 µm follows a mixed trend meaning that even the condensated vapor coating contains quite numerous small pores.

3.2 Classical post treatment

Cross section and surface pictures of as sprayed coating (FRONT region only) and post treated coating are displayed in Fig 9. A mix in between lamellar and vapor is observed in both, the post treatment involved in reducing the porosity from 2% to less than 0.7% mostly due to the disappearance of the smaller pores or the decrease in size of the bigger ones (almost by twice from 100 to 50nm). Regarding the surface analysis, it can be observed that well dispersed nanoparticles were generated during the post treatment induced by the following stages of diffusion, recrystallization and grain growth during the post treatment successively; both leading to densify the coating finally.

Fig 10 shows XRD patterns of that previous coatings. The mass ratio of each phase is listed in Table 3 based on Rietveld analysis. It can be seen that the TiO_2 formation is worth promoting by the post treatment according to the increase of its peak intensity, the rutile phase raised from 19.8% to 43.4% after post treatment respectively. The amount of intermediate phases such as Ti_2O, Ti_2O_3, Ti_3O or Ti_6O is strongly reduced accordingly. Due to their reactions with O_2 at low temperature, these intermediate phases contribute to reinforce TiO_2 phase. Then, microhardness and Young Modulus raised from 6.8 to 12.9GPa and from 115.3 to 191.1GPa respectively. As already mentioned by [22], the first diffusion stage induced a decrease of the porosity hence an increase of the hardness, the second recrystallization stage led to decrease the grains size and increase the TiO_2 phase ratio. Both of them contributed finally to the strengthening of such coatings.

The denser post treated coating associated with finer microstructure found on the surface and inside results in increasing mechanical properties.

4. Discussion

At first, it is worth noting a strong link between the coating microstructure and the particles flux when the substrate is partially protected from the direct plasma spray. The consequence is a clear change from mix lamellar/ columnar structure to a unique columnar structure. That can be attributed to first the propagation of the kinetic flux parallel to the surface and second to the transportation / condensation of the vapor carried by the flux on the hidden part of the substrate.

After in situ oxidation post treatment by R-VLPPS, the enhancement of the rutile TiO_2 phase in all the coatings can be observed: the amount of TiO_2 get higher with 92.4 wt% in the mainly lamellar structure coating and almost 100 wt% in the columnar structure. That confirms the efficiency of R-VLPPS post treatment to further oxidation mechanisms of Ti powder. Finally, pure TiO_2 thin film with low porosity and homogeneous thickness can be reached by that way.

The second oxidation post treatment via air gave rise to diffusion phenomena followed by recrystallization and grain growth of the nanoparticles inside the coatings. It allows their densification through the decrease of bigger pores and elimination of smaller ones. The coatings were composed of about 98 wt% TiO_2 phase inducing the increase of both hardness and Young modulus. Compared to the best results obtained by the first in situ post treatment (10.2GPa for hardness and 139.9GPa for Young Modulus), this post treatment could mainly be used to reinforce the mechanical properties of the coatings.

5. Conclusion

In situ R-VLPPS and air post treatment methods were applied on TiO_2 coatings sprayed via R-VLPPS. The results could be summarized as follows:

- An increase of TiO_2 amount was observed in the coatings whatever the post treatment method. Oxidation reactions were generated during in flight powder and on substrate surface. Oxidation mechanisms carried through the surface of the Ti powder are based on diffusion phenomena of O_2 inside the particles and between the coating layers.
- 100% TiO_2 phase could be obtained by in situ R-VLPPS post treatment in a vapor made coating. This method allows to manufacture rapidly homogeneous thin films of TiO_2.
- Denser coatings with greater hardness and Young modulus were achieved with classical oven air post treatment due to diffusion, recrystallization and grain growth phenomena. This method is a good alternative to increase mechanical properties.

Acknowledgements

The authors are grateful to the financial supports by Bourgogne Franche Comte Region [Grant N° 2019-7-09410]

Reference list

[1] M. Smith et al, Coatings, Vol 1(2), 2011, P 117-132

[2] K. Von Niessen et al, Thermal Spray Technology, Vol 19(1-2), 2010, P. 502-509

[3] A. Refke et al, B.R. Marple, C. Moreau (Eds.), Thermal Spray 2003: Advancing the Science and Applying the Technology, ASM International, Materials Park, OH, USA (2003), P. 581-588

[4] E.J. Young et al, Thin Solid Films, Vol 377–378, 2000, P. 788-792

[5] N. Zhang et al, Thermal Spray Technology, Vol 20(1-2), 2011, P. 351- 357

[6] M. Goral et al, Solid State Phenomena, Vol. 197 (2013) pp 1-5

[7] F. Sun et al, Power Sources, Vol 223, 2013, P. 36-41

[8] D. Marcano et al, Surface and Coatings Technology, Vol 318, 2017, P. 170-177

[9] B. Vautherin et al, Surface and Coatings Technology, Vol 275, 2015, P. 341-348

[10] C. Song et al, Material Letters, Vol 217, 2018, P. 127-130

[11] A. Fujishima et al, Nature, Vol 238, 1972, P. 37

[12] M. Adachi et al, Electrochem. Soc., Vol 150, 2003, P. 488

[13] Y. Evtushenko et al, Physics Procedia, Vol 73, 2015, P. 100-107

[14] A. Bendavida et al, Thin Solid Films, Vol. 355–356, 1999, P. 6-11

[15] J. Wang et al , European Ceramic Society, Vol. 38 (7), 2018, P. 2841-2850

[16] J. Waszko et al, Surface and Coatings Technology, Vol. 201 (6), 2006, P. 3443-3451

[17] L. Guo et al, European Ceramic Society, Vol. 37 (13), 2017, P.4163-4169

[18] H. Dong et al, Surf. Engineering, Vol 13(5), 1997, P. 402- 406

[19] P. Dearnley et al, Wear, Vol 256(5), 2004, P. 469-479

[20] X. Fan et al, in Proceedings of the International Thermal Spray Conference 2019, ITSC 2019, (eds)F. Azarmi and al, 26-29 May 2019, Yokahama, Japan

[21] J. Ilavsky et al, Appl. Crystallogr., 2018, Vol 51(3), p 867-882

[23] G. Mauer et al., Surf. Coat. Technol., Vol 220, 2013, P. 40-43

[24] X. Liu et al., Biomaterials, Vol 26(31), 2005, P. 6143-6150

[25] X. Zhao et al., Surf. Coat. Technol., Vol 201(15), 2007, P. 6878-6881

[26] A. Ohmori et al., Thin Solid Films, Vol 201(1), 1991, P. 1-8

[27] S. L. Tang et al., Materials Chemistry and Physics, Vol 213, 2018, P. 538-547

[28] E. Jordan et al, Materials Science and Engineering A, Vol 301(1), 2001, P. 80-89

Tables

Table 1 : Working conditions for in situ plasma oxidation post treatment

Coating	**mask**
O_2 injection	**Torch**
Reactive gas O_2 ($L.min^{-1}$)	**8**
Spray distance (mm)	**900**
Substrate temperature during spraying and VLPPS post treatment (°C)	**700**
Powder feed rate ($g.min^{-1}$)	**1**
Spraying velocity ($mm.s^{-1}$)	**200**
Passes	**400**

Table 2 : TiO_2 and Ti_2O, Ti_3O intermediate phases average ratio in as sprayed coating and after R-VLPPS oxidation post treatment (FRONT, INTERMEDIATE and HIDDEN zones)

Phases	**As sprayed coating**	**Post treated coating**		
		FRONT	**INTERMEDIATE**	**HIDDEN**
TiO_2 (%)	38,6	59,3	84,9	100
Ti_2O (%)	26,1	22,5	15,1	0
Ti_3O (%)	35,3	18,2	0	0

Table 3: TiO_2, and Ti_2O, Ti_3O, Ti_2O_3 intermediate phases average ratio in as sprayed coating and after oxidation post treatment

Phases	**As sprayed coating**	**Post treated coating**
TiO_2 (%)	19,8	43,4
Ti_2O (%)	65,4	20,5
Ti_3O (%)		36,1
Ti_2O_3 (%)	14,8	

List of figure captions

Fig 1

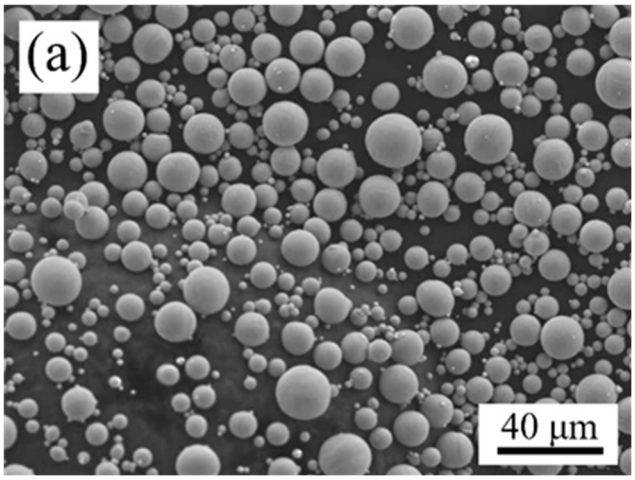

Fig 2

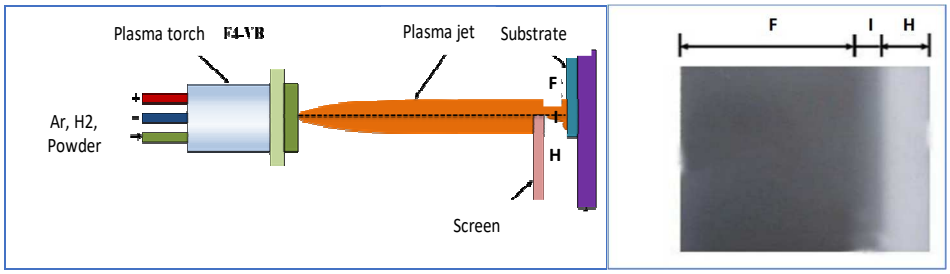
Plasma torch
F4-VB
Plasma jet
Substrate
Ar, H2,
Powder
F
H
Screen
F
I
H

Fig 3

FRONT	INTERMADIATE	HIDDEN
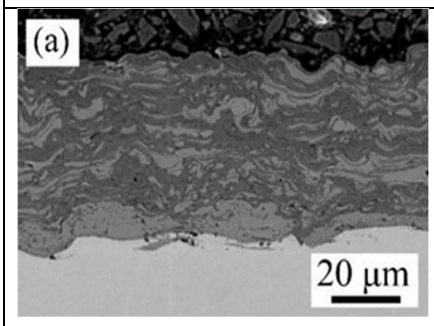	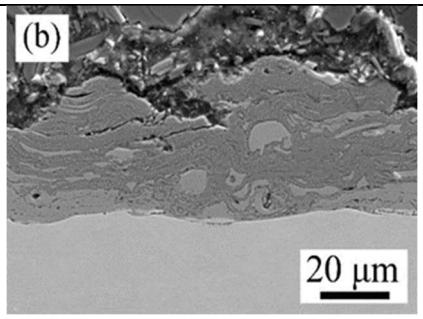	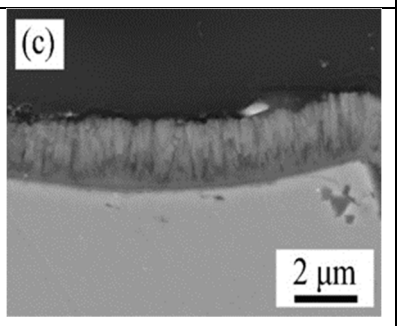

Fig 4

F : FRONT zone	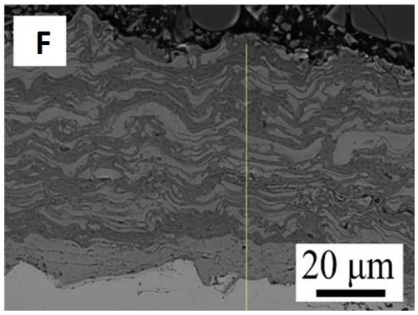	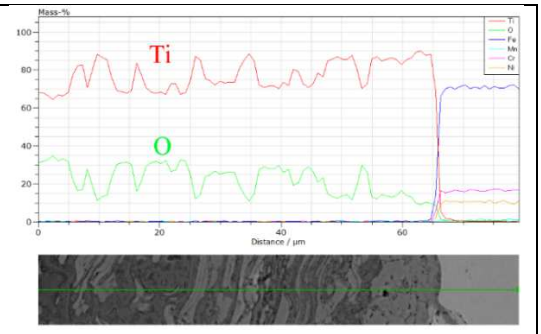
H : HIDDEN zone	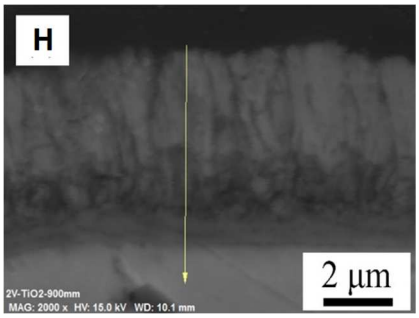	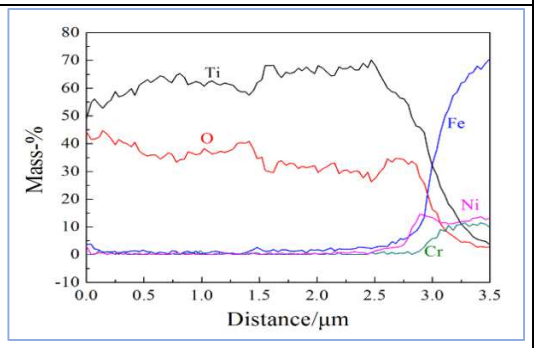

Fig 5

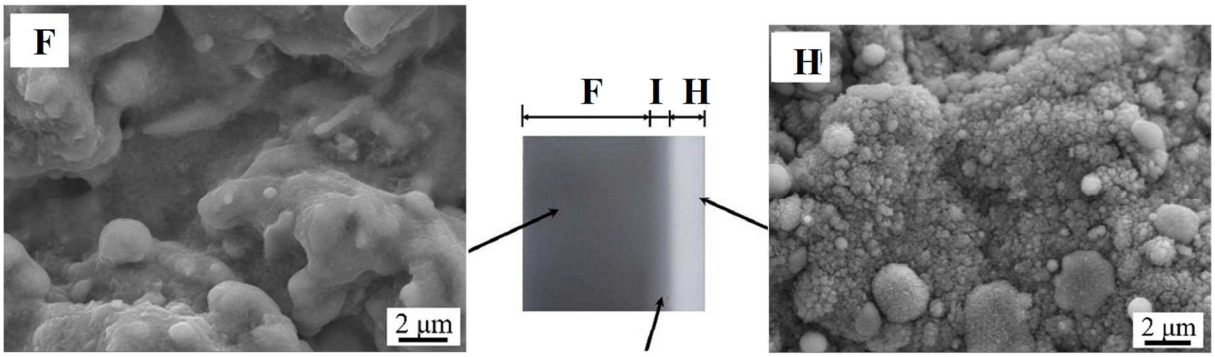

Fig 6

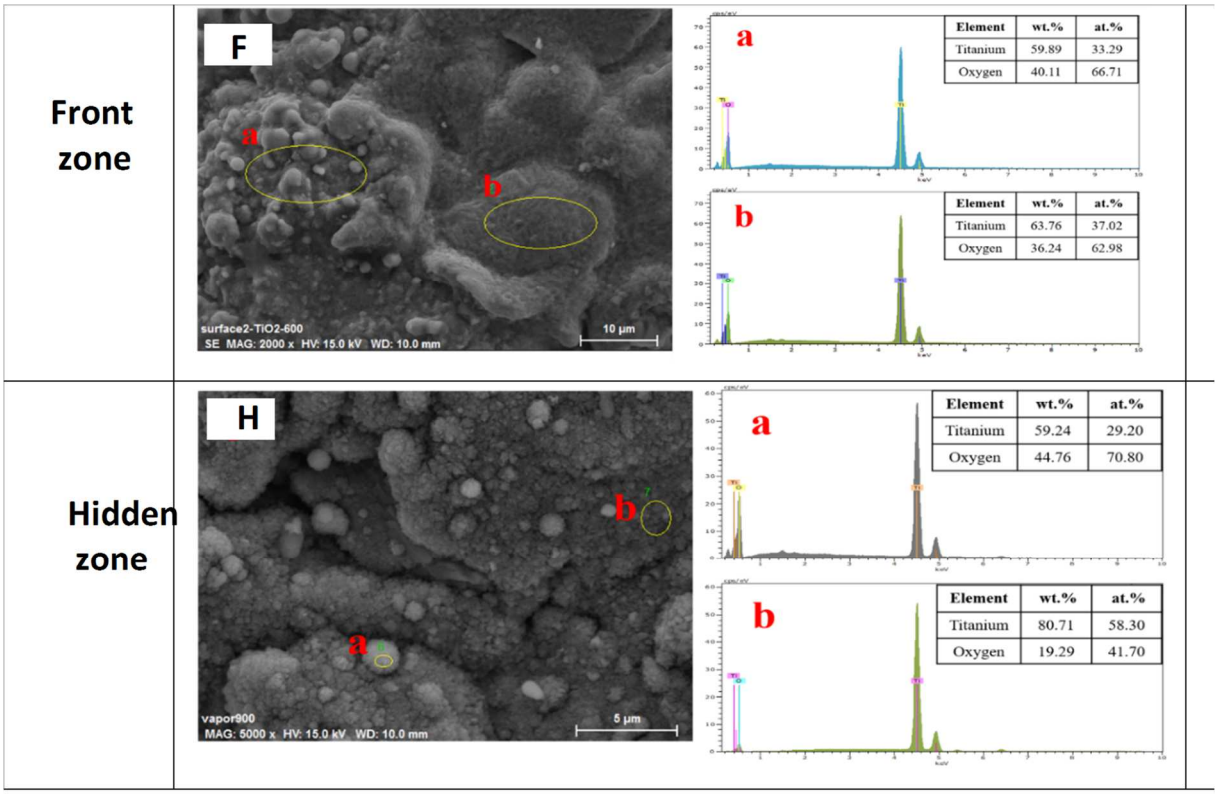
Front zone
F
a
b
surface2-TiO2-600
SE MAG: 2000 x HV: 15.0 kV WD: 10.0 mm
10 µm
a
Element wt.% at.%
Titanium 59.89 33.29
Oxygen 40.11 66.71
b
Element wt.% at.%
Titanium 63.76 37.02
Oxygen 36.24 62.98
Hidden zone
H
a
b
vapor900
MAG: 5000 x HV: 15.0 kV WD: 10.0 mm
5 µm
a
Element wt.% at.%
Titanium 59.24 29.20
Oxygen 44.76 70.80
b
Element wt.% at.%
Titanium 80.71 58.30
Oxygen 19.29 41.70

Fig 7

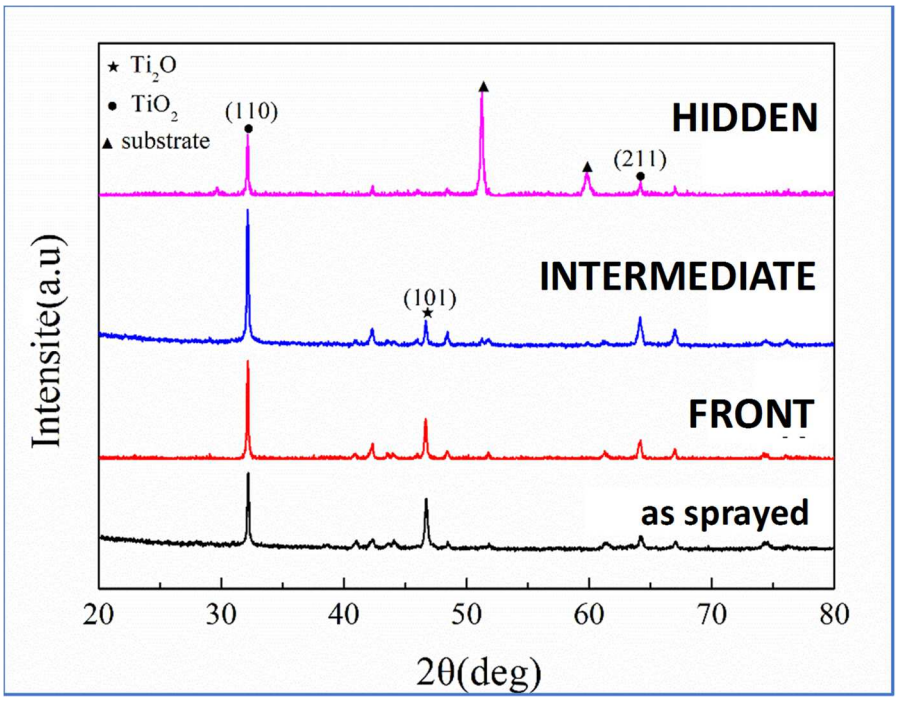
★ Ti2O
● TiO2
▲ substrate
(110)
(211)
(101)
HIDDEN
INTERMEDIATE
FRONT
as sprayed
Intensite(a.u)
20
30
40
50
60
70
80
2θ(deg)

Fig 8

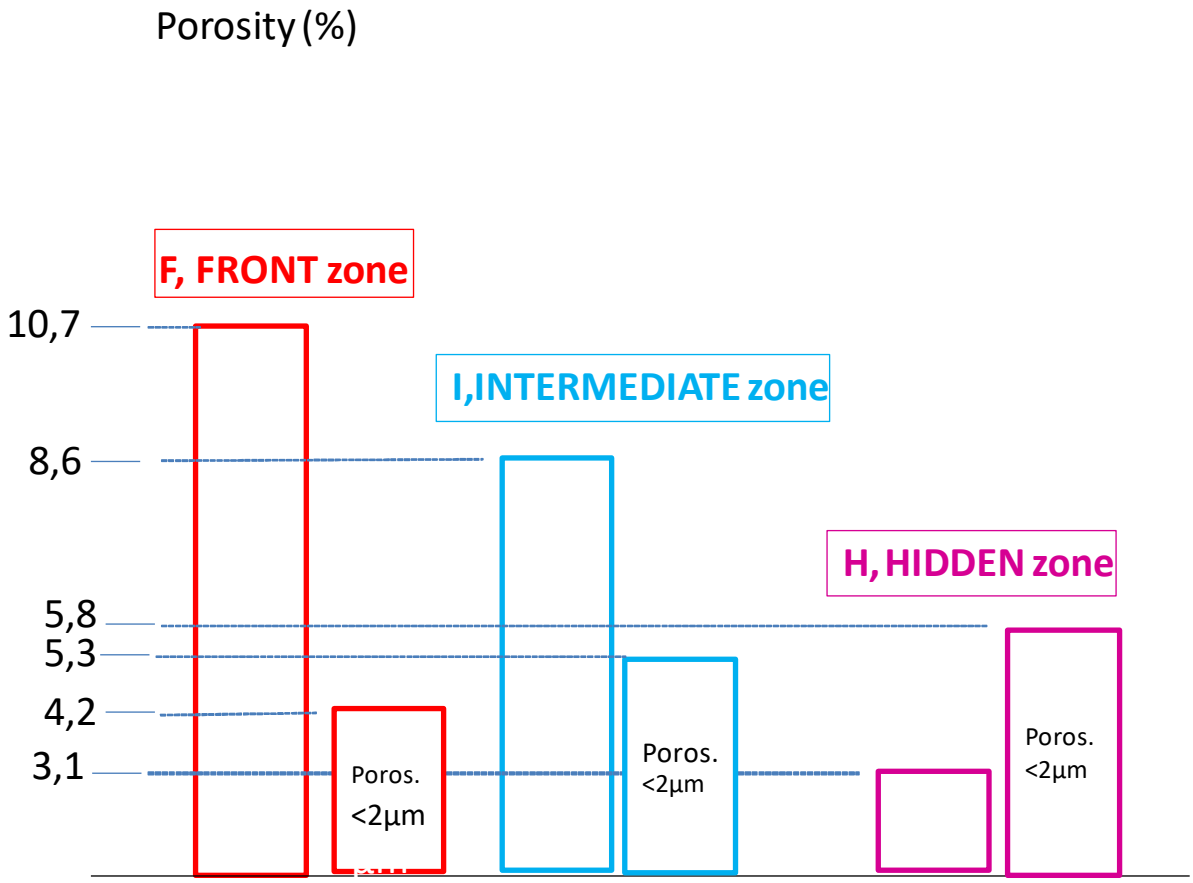
Porosity (%)
F, FRONT zone
10,7
8,6
5,8
5,3
4,2
3,1
Poros. <2µm
I,INTERMEDIATE zone
Poros. <2µm
H, HIDDEN zone
Poros. <2µm

Fig 9

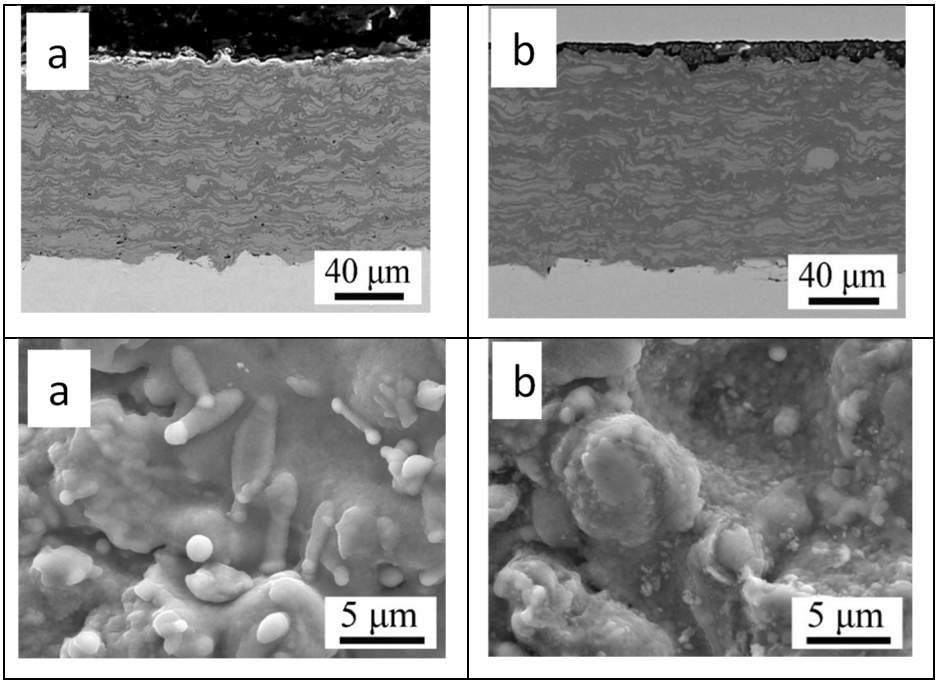

Fig 10

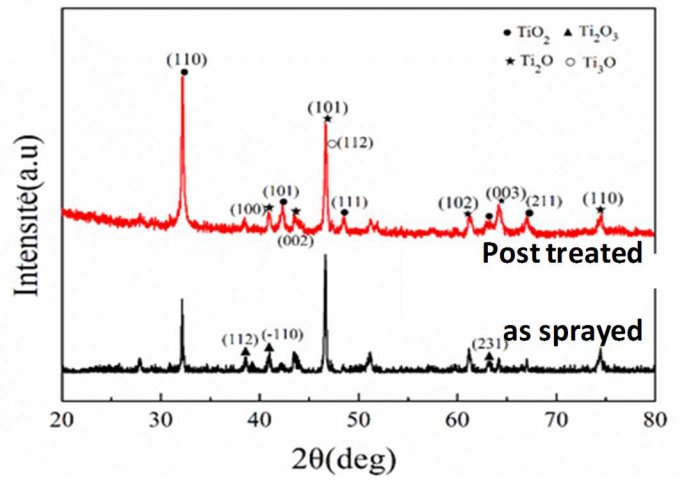
• TiO2 ▲ Ti2O3
★ Ti2O ○ Ti3O
(110)
(101)
(112)
(101)
(100)
(002)
(111)
(102)
(003)
(211)
(110)
Post treated
(112)
(-110)
(231)
as sprayed
Intensité(a.u)
20
30
40
50
60
70
80
2θ(deg)